

Laser-induced atmospheric Cu_xO formation on copper surface with enhanced electrochemical performance for non-enzymatic glucose sensing

Sotoudeh Sedaghat^{a,b}, Sina Nejati^{a,b}, Luis Regalada Bermejo^{a,b}, Zihao He^c, Alejandro M. Alcaraz^a, Alexander Roth^{a,d}, Zheng Li^e, Vilas G. Pol^e, Haiyan Wang^{a,c}, Rahim Rahimi^{a,b*}

^a Birck Nanotechnology Center, Purdue University, West Lafayette, IN, 47907, USA

^b School of Materials Engineering, Purdue University, West Lafayette, IN, 47907, USA

^c School of Electrical and Computer Engineering, Purdue University, West Lafayette, IN, 47907, USA

^d School of Mechanical Engineering, Purdue University, West Lafayette, IN, 47907, USA

^e Davidson School of Chemical Engineering, Purdue University, West Lafayette, IN 47907, USA

Emails: ssedagha@purdue.edu (S. Sedaghat), snejati@purdue.edu (S. Nejati), lregalad@purdue.edu (L. Regalado Bermejo), he468@purdue.edu (Z. He), alcarazr@purdue.edu (A. M. Alcaraz), roth70@purdue.edu (A. Roth), li3259@purdue.edu (Z. Li), vpol@purdue.edu (V. G. Pol), hwang00@purdue.edu (H. Wang), rrahimi@purdue.edu (R. Rahimi)

1. Fabrication of LIO-Cu Electrode

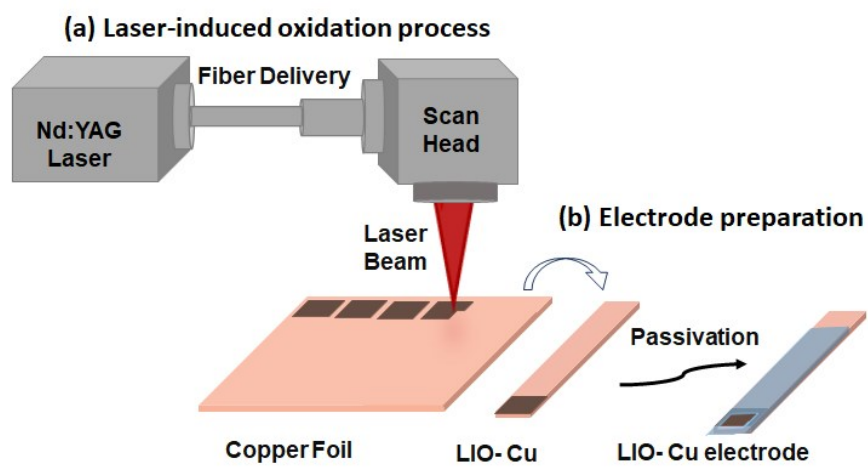


Fig. S1. Schematic illustration of LIO-Cu electrode fabrication.

2. GI-XRD analysis using different incident beam angles

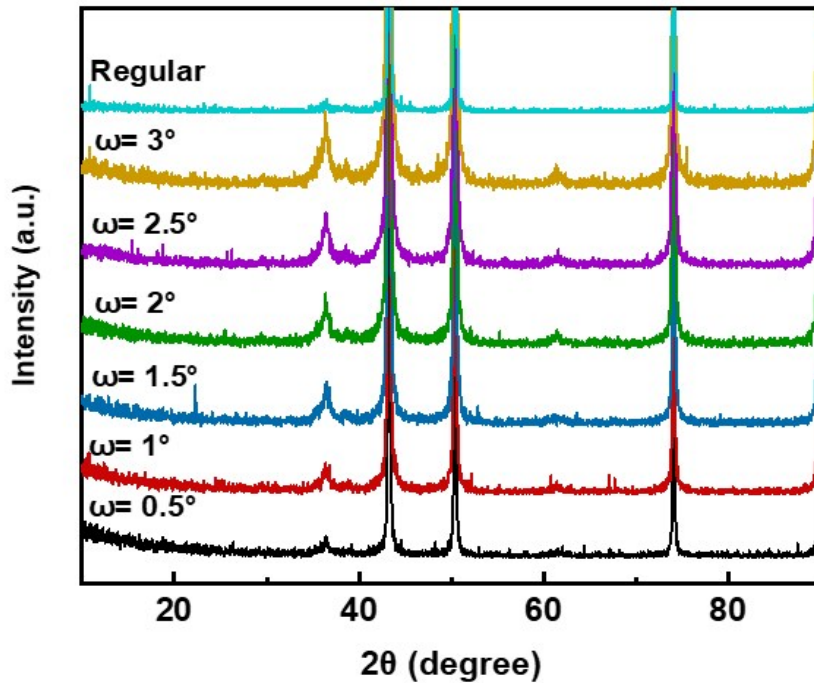


Fig. S2. GI-XRD data using different incident beam angles.

3. Particle Size Distribution of LIO-Cu structures

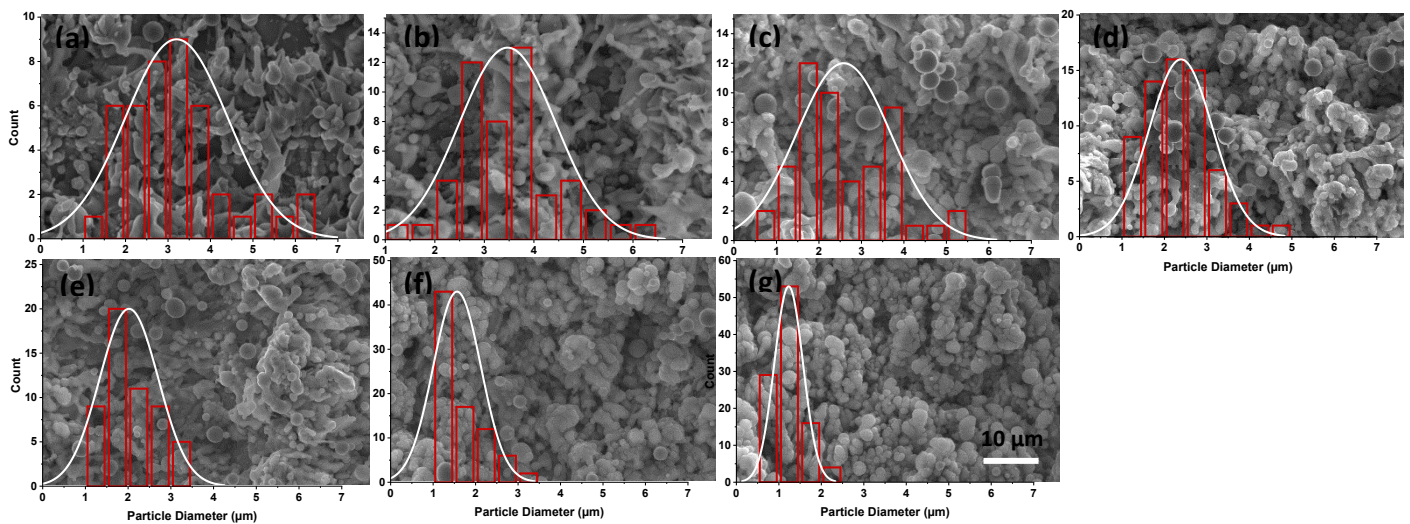


Fig. S3. FE-SEM micrographs and particle size normal distribution of LIO-Cu surfaces fabricated using different laser powers of (a) 16 W, (b) 16 W (c) 20 W, (d) 24 W, (e) 28 W, (f) 32 W, (g) 36 W, (h) 40 W.

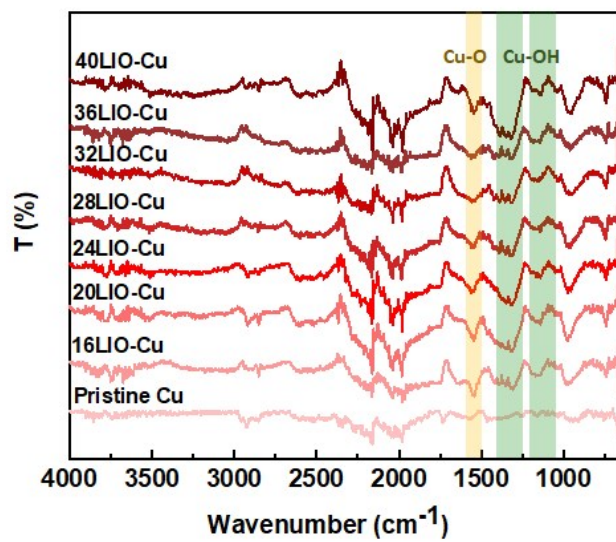


Fig. S4. ATR-FTIR spectra of pristine and different LIO- Cu samples.

4. ATR-FTIR analysis of pristine and LIO-Cu samples

5. LIO-Cu surface profile and profilometry data

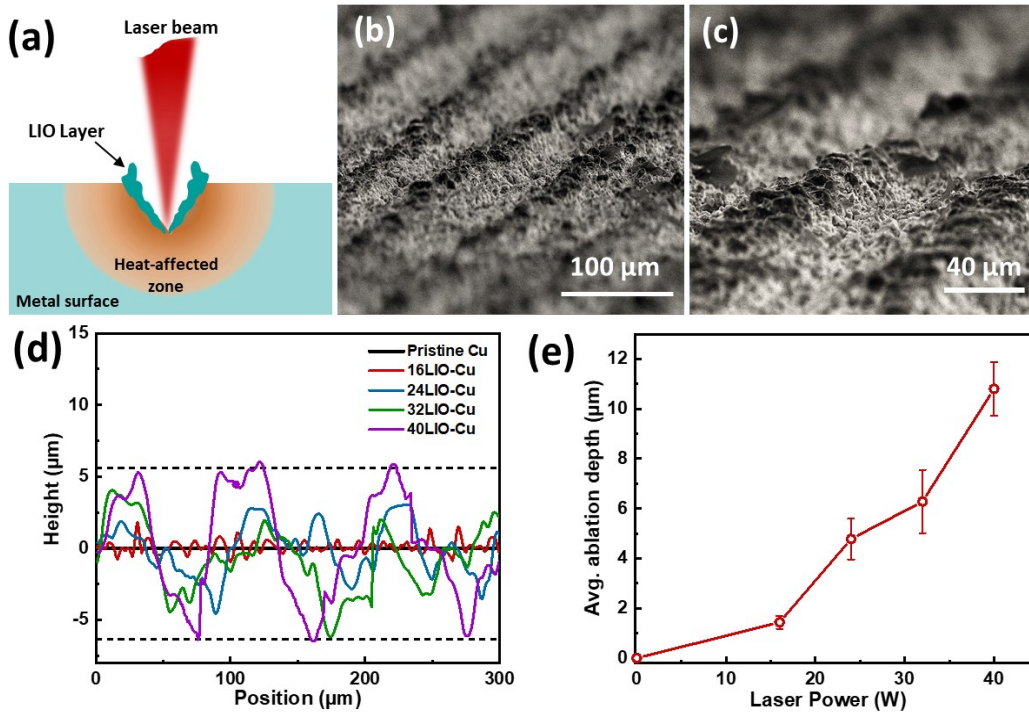


Fig. S5. (a) schematic illustration of the heat-affected zone of laser beam. (b and c) SEM images of 40LIO-Cu surface. (d) Profilometry data, and (e) change in the average ablation depth calculated from profilometry data for pristine and different LIO-Cu samples.

6. Surface roughness and wettability properties of pristine and LIO-Cu samples

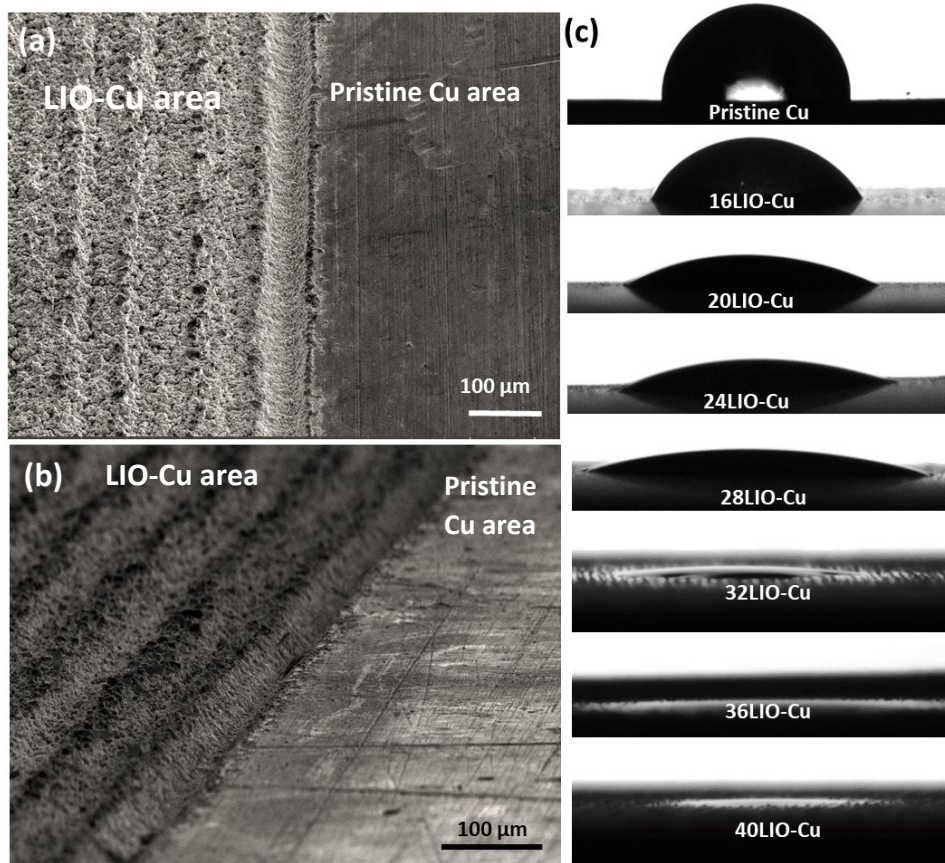


Fig. S6. (a, and b) SEM images of the 40LIO and pristine Cu structure showing the roughness of LIO-Cu structure. (c) Wetting properties of pristine-Cu and different LIO-Cu samples studied by water contact angle measurement.

For further analysis of surface roughness, we performed surface wettability analysis of the laser processed copper surfaces using water contact angle measurement. These results showed a clear decrease in the contact angle values by increasing the laser processing power which further confirm the increase surface roughness at higher laser processing powers. This observation can be explained by the Wenzel theory² which describes the relationship between surface roughness and contact angle:

$$\cos \theta^* = r \cdot \cos \theta$$

θ^* = Measured (apparent) contact angle processed surface

θ = Contact angle on the smooth surface

r = Surface roughness coefficient

Given the hydrophilic properties for pristine coppers surfaces ($CA < 90^\circ$) the surface is even more wettable with increasing surface roughness through laser processing.

In our case, the concurrent formation of high surface roughness and high contents of hydrophilic copper oxide compounds created on the laser processed surface both help in creating a highly energetically favorable surface to water. As shown in **Fig S6** copper surface that were processed with laser powers greater than 36W had a superhydrophilic surface property ($CA < 5^\circ$).

7. Glucose Oxidation mechanism on LIO-Cu

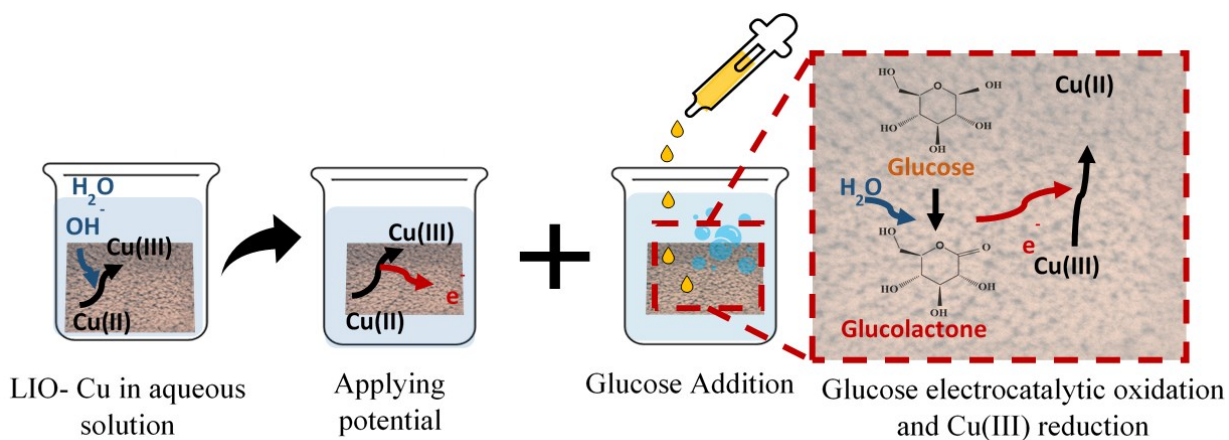


Fig. S7. Schematic of LIO-Cu behavior in aqueous solution and glucose determination mechanism on its surface.¹

8. Glucose detection response on 40LIO-Cu using different applied potentials

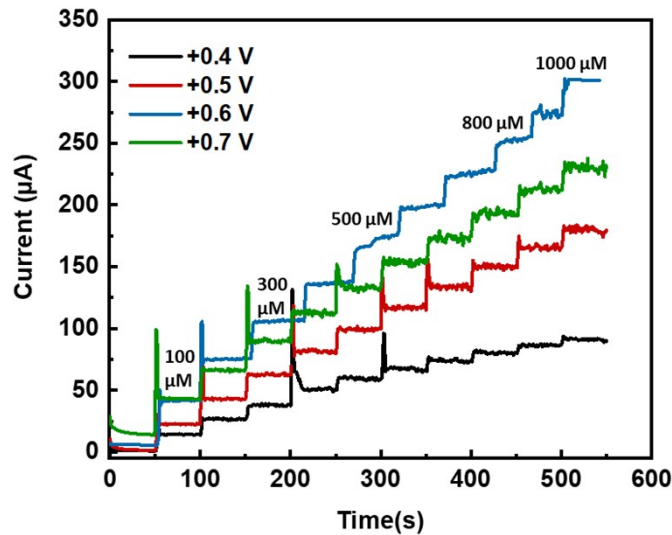


Fig. S8. Amperometric response of 40LIO-Cu electrode toward successive glucose addition in different applied potentials.

9. Cost estimation of the developed LIO-Cu sensor:

The cost estimation as of 2021 for manufacturing of our sensors were based the estimated cost of copper foil (\$26 per 20 cm × 100 cm), power cost of operating the laser ULS system (\$5 per hour with considering the constant electricity and maintenance of the system), and silicone passivation material used in packaging of the sensor (\$2.8 per kilogram).

The estimated cost for each sensor is provided as below:

In this process we used 99.9% copper sheets with thickness of 0.05mm and priced at \$26 for a total area of 20 cm × 100 cm = 2000 cm²

Therefore, the cost of copper foil for each cm² was approximated at \$0.013/cm².

Dimension of each electrode we fabricated was: 50 mm (L) × 4 mm (W) = 200 mm² = 2 cm²

Therefore, the total cost of copper used in fabrication of the sensor was:

Cost of copper material per electrode: ($\$0.013 / \text{cm}^2$) × 2 cm² = \$0.026 = 2.6 cents

The time required for laser processing the copper surface was less than 2 seconds. Therefore, the cost for laser processing was estimated at:

Laser processing cost per electrode: $(\$5/h) \times 2 \text{ s} = \$0.0027 \approx 0.3 \text{ cents}$

The estimated amount of silicone glue used in passivation of each individual electrode was about 0.1 grams. Therefore, the cost for packaging of the sensor was estimated at:

Packing cost per electrode: $(\$2.8/Kg) \times 0.1 \text{ grams} = \$0.0028 \approx 0.3 \text{ cents}$

The total cost of each glucose sensor using our demonstrated laser processing approach was estimated to be around 3.2 cents. The estimated cost of these sensors was significantly lower than the enzymatic counterparts. Rough retail costs per of commercially available glucose test strips are about \$0.9 - \$1.2 per strip (One Touch Ultra strips- BKT Glucose Test Strips).

It should be noted that many of the estimated costs for our demonstrated glucose sensor can be significantly reduced by utilizing industrial scale roll-to-roll laser processing machines with faster processing time and purchasing bulk copper foil roles for scale up production³.

References

1. S. Sedaghat, C. R. Piepenburg, A. Zareei, Z. Qi, S. Peana, H. Wang and R. Rahimi, *ACS Applied Nano Materials*, 2020.
2. K. Kubiak, M. Wilson, T. Mathia and P. Carval, *Wear*, 2011, **271**, 523-528.
3. R. Rahimi, M. Ochoa and B. Ziaie, *ACS applied materials & interfaces*, 2018, **10**, 36332-36341.